

Test and Simulation of the Positron Converter for the SPring-8 Linac

Akihiko MIZUNO, Shinsuke SUZUKI, Hiroshi YOSHIKAWA,
Toshihiko HORI, Kenichi YANAGIDA, Kenji TAMEZANE, and Hideaki YOKOMIZO
JAERI-RIKEN SPring-8 Project team
2-28-8 Honkomagome, Bunkyo-ku, Tokyo

Abstract

For designing an electron/positron converter (target and focusing system) for the SPring-8 Linac, we constructed a test apparatus in Tokai Establishment, and obtained energy spectrums of the generated positrons with various parameters of focusing system. Also, we developed a simulation code of tracking particles in the positron focusing section.

Though the test apparatus is simple compared with the planed one for the SPring-8 Linac, we obtained conversion efficiency of 0.27% after the focusing section. The dependence of the experimental results on parameters of focusing system are coincident with that of simulation one.

I. INTRODUCTION

We are planning to use positrons for SPring-8 Linac to avoid the ion-trapping in a storage-ring. The positrons will be generated in the linac at 250MeV section, and accelerated up to 900MeV at the end of the linac. For getting high intensity light from the storage-ring, we have to achieve high conversion efficiency as possible.

The injection part of the linac (from electron gun to bunching section) has been already constructed, and it's commissioning is under way. In the test of the 40nsec pulse widths mode with cathode assembly of "Y-796", we obtained the current of 12A at the end of the bunching section, and of the 1nsec mode, 22A[1].

In order to achieve high conversion efficiency of SPring-8 Linac, we constructed the test apparatus of positron generator and focusing system in Tokai Establishment. And also we developed a code of electron/positron converter for simulating the test apparatus in various parameters.

In this paper, we present the results of experiment and simulation, and a simulation data of a improved focusing system.

II. OUTLINE OF APPARATUS AND SIMULATION

A. The Test Apparatus

A test apparatus is constructed and installed in a beam line of JAERI-linac. The apparatus (see FIG.1) consists of a removable tungsten target (insert or pull out), focusing section (one pulse-solenoidal coil, one DC1-coil, one DC2-coil, one S band accelerator structure and one quadrupole magnet), and measurement section (energy analysis magnet and Faraday cup). Electrons bombard to the target with an energy of about

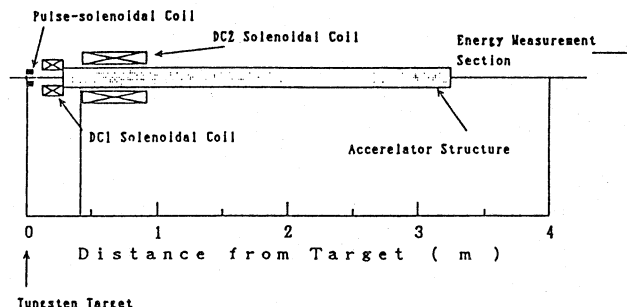


FIG.1 The outline of the test apparatus

100MeV. Generated positrons are focused and accelerated up to ~35MeV in the focusing section. The energy of the positrons are measured by the analyzer composed of a 90°magnet and a Faraday cup.

B. Simulation Code

Calculations for this experiment are using two codes. One is EGS4" (Electron Gamma Shower version.4)[2] for positron generation at the tungsten target. And the other is our original code for tracking through the focusing section.

In the EGS4 simulation, we assumed the profile, radius, and injection angle of the injected electron beam for the initial condition. Conditions of the target are same as that of in experiment. The initial conditions of EGS4 are shown in TABLE.1.

TABLE.1 Conditions for EGS4 Calculation

Injected electron energy	120MeV
Injected beam radius	1.0mm
Injection angle to the target	0 rad
The number of injected electrons	1,026,000
Profile of electrons	Gaussian distribution
Target	Tungsten
Target figure	Circular plate
Target radius	10.0mm
Target thickness	6.0mm

EGS4 provides tracking code the initial conditions of positrons; such as energy, direction and radial position on the surface of the target.

The tracking code is based on the forth-ordered Runge-Kutta method for calculating Maxwell equations in the electromagnetic field of the focusing section. Since positron currents are low (~10mA in the SPring-8 linac), we neglected

Coulomb interactions between positrons. So each ray trace is independent, we calculated in parallel by vector processor, VP2600, at Computing and Information Center JAERI.

The magnetic field is caused by the solenoidal coils. We adopted calculated longitudinal and radial magnetic fields along the beam line in the focusing section with assumption that cylindrical currents flow at the positions of the coils. Longitudinal magnetic field is shown in FIG.2 at the case of the strongest fields in the experiment, currents of coils are 5.8kA(pulse-solenoidal coil), 350A(DC1 coil), and 130A(DC2 coil) respectively.

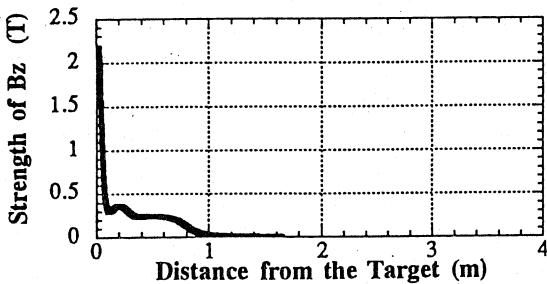


FIG.2 Longitudinal magnetic field along the beam line

The electric field is caused by the accelerator structure. In this experiment, positrons with an energy of around 10MeV at the surface of the target are mainly collected. So their speed is almost equal to light speed, we assume that static field exists in the area of the accelerator structure.

In this code, the positrons are tracked to the finishing point of 4 meters from the target, around energy analysis magnet. During tracking through focusing section, we discard positrons which radial position is more than 17 mm away from the center axis.

III. RESULTS OF EXPERIMENT AND SIMULATION

In the following, we show the experimental data compared with the simulation one. Varied parameters are currents of the solenoidal coil (2.0kA, 4.0kA, 5.8kA), DC1 coil (0A, 200A, 350A), and DC2 coil (0A, 50A, 130A). Other parameters are fixed. TABLE.2 shows parameters of this experiment.

A. Pulse-Solenoidal Coil

At first we show effects of the pulse-solenoidal coil in FIG.3 (a) (experiment) and (b) (simulation). The data are energy spectrums of positrons at the Faraday-cup(experiment) or at the finishing point(simulation). In experimental data, the abscissa represents an output current of the energy analysis magnet, and the ordinate is a signal from the Faraday-cup. Their energy resolution is wider at the right side of abscissa. Also in the simulation data, energy resolution is proportional to positron energy, and ordinates are arbitrary unit.

In FIG.3, global shape of spectrums and relative intensity of the positron current are similar in (a) and (b). We know that peaks in the spectrums due to the pulse-

TABLE.2 Parameters of Experiment

FIXED	
Target	see TABLE.1
Injection electron current	150nA(average)
Injected electron energy	90MeV
Repetition rate	5pps
Pulse width of injected current	1μsec
Energy gain in the accelerator structure	33.1MeV
VARIABLE	
Pulse-solenoidal coil	2.0kA, 4.0kA, 5.8kA
DC1 coil	0A, 200A, 350A
DC2 coil	0A, 50A, 130A

solenoidal coil sift with current of pulse-solenoidal coil. Besides, peak due to other coils don't sift with current of pulse or other coils.[3] In FIG.3, a peak of lower energy corresponds to the pulse-solenoidal coil because it sifts with pulse-solenoidal coil current. And a peak of higher energy is due to other coils; DC1 or DC2, because it does not sift. In the bottom figure, two peaks become same position in abscissa, and form only one peak. These are coincident between (a) and (b).

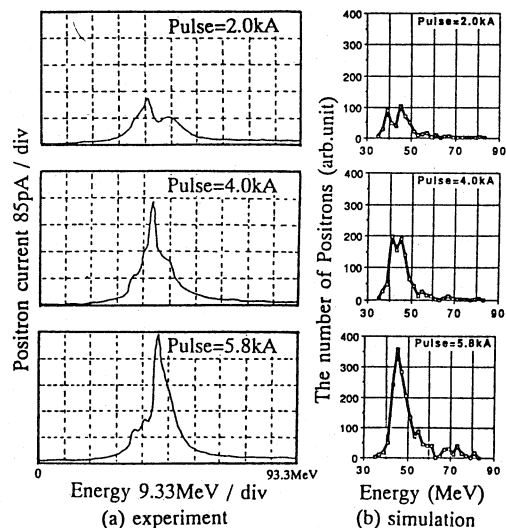


FIG.3 effect of pulse-solenoidal coil
DC1=350A DC2=130A

B. DC1 Coil

The results with various currents of DC1 coil are shown in FIG.4 (a) and (b). The global shapes of spectrums are quite similar in (a) and (b), but relative intensities of positrons are different. Perhaps, there are some misalignment between pulse-solenoidal coil and DC1 coil, or detail figures of this section are different between experiment and simulation.

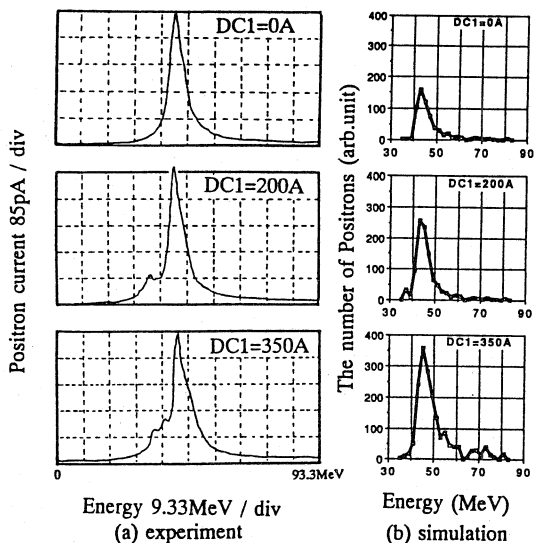


FIG.4 effect of DC1 solenoidal coil
Pulse=5.8kA DC2=130A

C. DC2 Coil

FIG.5 (a) and (b) show the dependencies of the current of DC2 coil. Both global figures of spectrums and the relative intensities of the positrons are similar between (a) and (b). Especially position of small peaks in the abscissa (perhaps due to DC1 coil) are coincident.

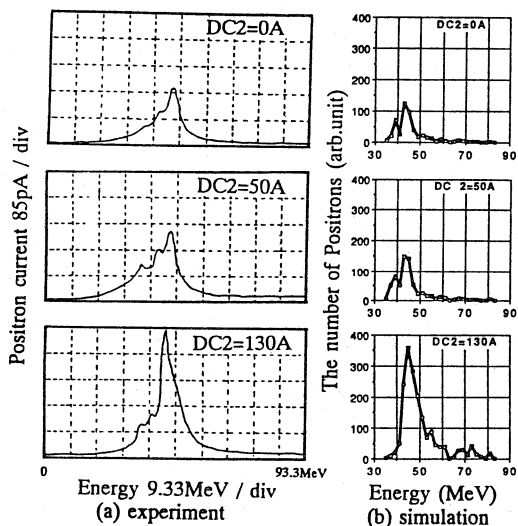


FIG.5 effect of DC2 solenoidal coil
Pulse=5.8kA DC1=350A

In the conditions of bottom one in the above figure, the conversion efficiency (peak current of the obtained spectrum versus that of the injection one) is 0.27% in experiment. On the other hand in simulation, it's 0.11% (the number of obtained particles versus that of injection one). Their difference causes from the difference of detail parameters between experiment and simulation. So we can understand only

variational tendency of global figure of spectrums or positron intensity from these results.

D. Simulation of a improved geometry

We examined the simulation of a improved geometry by this simulation code[3]. This system has 6 DC2 solenoidal coils mounted over the accelerator structure. The energy gain in the accelerator structure is 40MeV, and the magnetic field of this condition along the beam line is shown in FIG.6. Except the energy gain and the magnetic field, the conditions are similar to these of FIG.3 ~ 5. In this case, we obtained the conversion ratio to be 0.45% at the end of first accelerator structure. From these results, we can expect the efficiency to be more than 0.45% at the end of the first accelerator structure in the SPring-8.

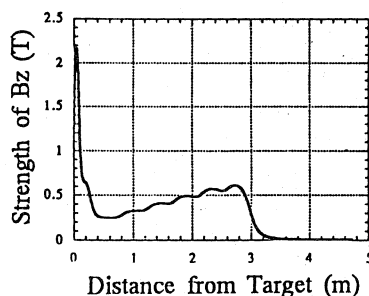


FIG.6 Magnetic field of improved geometry

IV. CONCLUSION

For designing the electron/positron convertor for SPring-8 Linac, we constructed the test apparatus and developed the simulation code. Experimental data are qualitatively explained by the prediction obtained from a simulation code.

In the experiment, we obtained the conversion efficiency to be 0.27%. From this result and the simulation, we can expect the conversion efficiency to be over 0.45% at the end of the first accelerator structure in the SPring-8 Linac.

V. REFERENCES

- [1] S.Suzuki et al., "Initial data of Linac Preinjector for SPring-8," 1993 PARTICLE ACCELERATOR CONFERENCE, Washington, D.C., Omni Shoreham Hotel, May, 1993
- [2] Walter R.Nelson, Hideo Hirayama and David W.O.Rogers, "THE EGS4 CODE SYSTEM", SLAC-Report-265, 1985
- [3] A.Mizuno et al., "Simulation of Electron-positron Convertor for SPring-8", JAERI-M report 93-030